

Design of a large displacement thermal actuator with a cascaded V-beam amplification for MEMS safety-and-arming devices

Xiuyuan Li · Yulong Zhao · Tengjiang Hu ·
Wenju Xu · You Zhao · Yingwei Bai · Wei Ren

Received: 12 September 2014 / Accepted: 21 January 2015 / Published online: 7 February 2015
© Springer-Verlag Berlin Heidelberg 2015

Abstract The design, fabrication and characterization of a large displacement thermal actuator with a cascaded V-beam amplification for MEMS safety-and-arming (SA) devices are presented. The device is comprised of two V-shape electrothermal actuators, a cascaded V-beam amplification and two mechanical sliders. Compared with conventional lever amplifications, the vertical anti-acceleration stiffness of V-beam amplifications is much larger, which can meet the need of high-acceleration weapons. The special design of two symmetric mechanical sliders can double the displacement to ensure the MEMS SA device in armed state. The whole device is fabricated on a SOI wafer and fabrication process is introduced. Under an applied voltage of 15 V, the displacement of the device is 231.78 μm with consuming power of 5.10 W and response time of 16 ms. The chip size of the actuator is about 4 mm \times 5 mm \times 0.5 mm. The proposed actuator possesses outstanding performance in miniaturization, low cost and easy integration with other parts of MEMS SA devices.

1 Introduction

Safety-and-arming (SA) devices are necessary components for munition fuzes to keep the detonator safe with mechanical sliders during transportation. Once the launch environment is detected, the SA device would arm the munition by moving away the sliders via an actuator (Robinson et al. 2005). The miniaturization of the actuator for SA devices contributes a lot to afford the diminishment in device volume, which promotes the system intelligence (Zunino et al. 2008). Weapons with smaller actuators can provide more space for sensors, power arrangement and signal electronics. However, most conventional actuators employing macro manufacturing processes are relatively bulky, expensive and difficult to integrate with MEMS SA devices.

In recent years, MEMS technologies have been adopted in the military field because MEMS devices may decrease in the volume, mass, cost and power consuming by a large margin (Pennarun et al. 2005). But most reported MEMS-based actuators for SA devices could not be widely used in small/medium caliber munitions because of the high fabrication cost by using LIGA technique (Fan et al. 1998), restriction in arming force and large volume induced by the driven structure (Maurer et al. 2006; Hélène et al. 2010). MEMS electrothermal actuators can generate a large force with small volume and cheap cost while the output displacement is small. In order to amplify the displacement, cascaded electrothermal actuators (Hill et al. 2006; Lai et al. 2006), racks (Maloney et al. 2004) and levers (Su and Yang 2001; Yang et al. 2009; Khazaai et al. 2010) are adopted in the reported papers, respectively. Vertical anti-acceleration stiffness is a key index of high-acceleration weapons and reflects the overload resistance of SA devices. Cascaded actuators and racks could not be used in weapons because of their small vertical anti-acceleration stiffness. Though

X. Li · Y. Zhao (✉) · T. Hu · W. Xu · Y. Zhao
State Key Laboratory of Manufacturing Systems Engineering,
Xi'an Jiaotong University, Xi'an 710049,
People's Republic of China
e-mail: zhaoyulong@mail.xjtu.edu.cn

X. Li
e-mail: xiuyuanjun@126.com

Y. Bai · W. Ren
Science and Technology on Applied Physical Chemistry
Laboratory, Shaanxi Applied Physical Chemistry Research
Institute, Xi'an 710061, People's Republic of China

the vertical anti-acceleration stiffness of levers is larger than cascaded actuators and racks, electrothermal actuators with levers are only fit for low-acceleration weapons.

Herein, a thermal actuator with a cascaded V-beam amplification is proposed for high-acceleration SA devices. Compared with conventional lever amplifications, the vertical anti-acceleration stiffness of V-beam amplifications is much larger, which is fit for high-acceleration weapons. The arming action is driven by two V-shape electrothermal actuators, which equip outstanding performance in miniaturization, low cost, low actuation voltage and easier integration with sophisticated components compared to electrostatic actuators (Deutschinger et al. 2010; Pustan et al. 2012). To meet the requirement of large displacement, two symmetric mechanical sliders are integrated to produce opposite movement. This special design of two reversed sliders can double the displacement to ensure the MEMS SA device in armed state.

2 Device description and analytical modeling

The schematic of the designed actuator for SA devices is shown in Fig. 1. The two V-shape electrothermal actuators are symmetric and provide displacement for the amplification. Two mechanical sliders are integrated with the actuator and closed to each other when the SA device is in safe state. When the launch environment is detected, voltage would be applied to the V-shape electrothermal actuators.

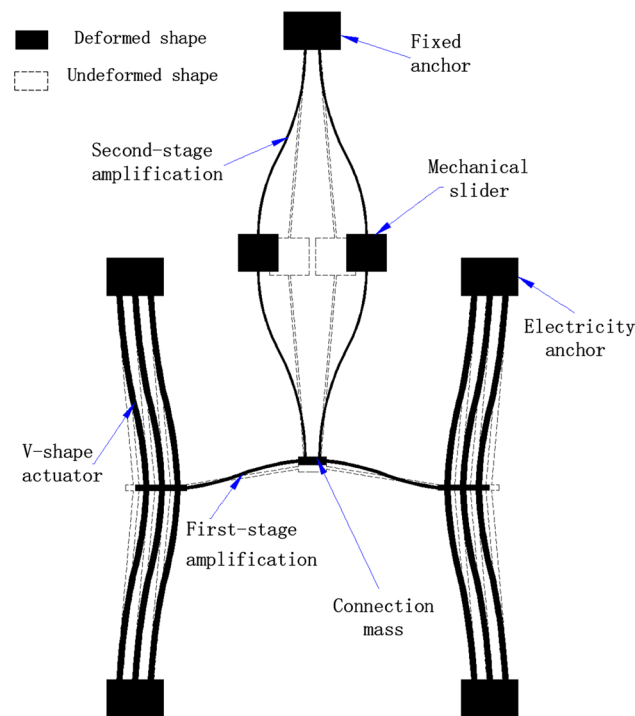


Fig. 1 The schematic of the designed actuator for SA devices

The first-stage amplification amplify the output displacement and push the connection mass upwards. Meanwhile, the second-stage amplification is compressed along the vertical direction and expanded in the horizontal direction. Thus, the two mechanical sliders move reversely to ensure the MEMS SA device in armed state.

2.1 Analytical modeling of an electrothermal V-shape actuator

Figure 2 shows the structure of an electrothermal V-shape actuator. The V-shape actuator can generate relevant heat when electric current passes through the beam. The heat transfer path in an electrothermal actuator is illustrated in Fig. 3. The length of the V-shape actuator is much larger than its cross section size. Thus, the heat analysis can be seen as a one dimensional heat diffusion problem (Enikov et al. 2005). The temperature distribution of the V-shape actuator can be obtained by the following equation:

$$k_s \frac{d^2 T(x)}{dx^2} + B^2 \rho = \frac{Sk_V}{h} \frac{T(x) - T_r}{t_V} \tag{1}$$

with the thermal boundary conditions:

$$T(0) = T(L) = T_r \tag{2}$$

where $S = \frac{h}{w} \left[\frac{2t_V}{h} + 1 \right] + 1$ and $B = \frac{V}{2\rho l}$. l_1 is the thermal conductivity of silicon. θ_1 is the voltage applied on the actuator. ρ is the electrical resistivity of silicon. h_1 is the thickness of the air gap. k_V is the thermal conductivity coefficient of the air gap. $K_{LM} = \frac{2\sigma J^2}{2L_L^2 + 2J^2 - 3L_L J}$ is the reference temperature and generally equals to the room temperature.

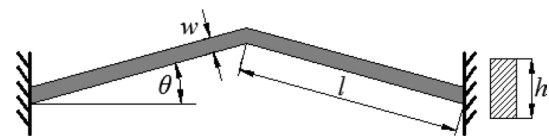


Fig. 2 The structure of an electrothermal V-shape actuator

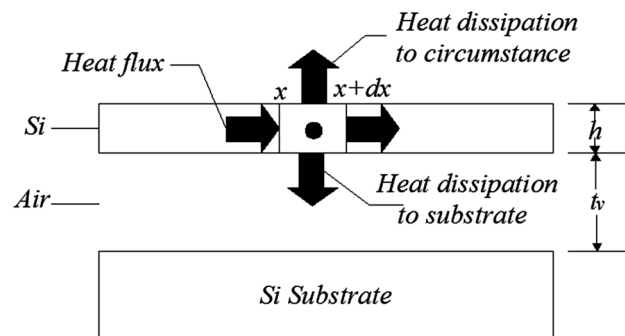


Fig. 3 The heat transfer path in an electrothermal actuator

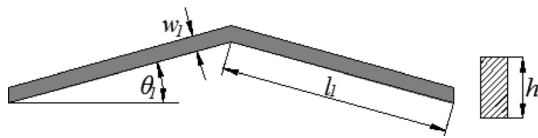


Fig. 4 The structure of a V-beam amplification

As the two ends of the V-shape actuator are anchored, thermal expansion caused by Joule heating pushes the apex outward, resulting in a rectilinear displacement. The maximum apex displacement of a V-shape actuator could be expressed as follows (Gianchandani and Najafi 1996):

$$d_{max} = \frac{\eta l \bar{T} \sin \theta}{(w/l)^2 + \sin^2 \theta} \tag{3}$$

where $\bar{T} = \frac{1}{2l \cos \theta} \int_0^{2l \cos \theta} T(x) dx$. η is the thermal expansion coefficient of the material.

The output stiffness k_{out} of a V-shape actuator can be calculated by the following equation when the beam slope is in the range of 0.05 ~ 0.2 rad (Long et al. 2001):

$$k_{out} = \frac{2 \sin^2 \theta w h E}{l} \tag{4}$$

where E is the Young’s modulus.

2.2 Analytical modeling of a cascaded V-beam amplification

By taking the system symmetry into account, the second-stage amplification can be simplified to a first-stage amplification under the same displacement on both sides. Thus, the first-stage amplification and second-stage one have the same operation principle. The first-stage amplification is taken as an example for the following theoretical analysis. The structure of a V-beam amplification is illustrated in Fig. 4.

2.2.1 Amplification factor of a V-beam amplification

In consideration that the displacement is large and the width of the V-beam is small (less than 20 μm), one half of the first-stage V-beam amplification can be regarded approximately as a triangulation amplification with hinges at the ends of the beam. The simplified model of one half of a V-beam amplification is shown as Fig. 5.

The mechanical amplification factor of a V-beam can be expressed by the geometric relationships as:

$$m = \frac{\Delta y_1}{\Delta x_1} = \frac{\sqrt{l_1^2 - (l_1 \cos \theta_1 - \Delta x_1)^2} - l_1 \sin \theta_1}{\Delta x_1} \tag{5}$$

The formulas obtained from analytical methods are then validated by finite element method ($l_1 = 1,000 \mu\text{m}$,

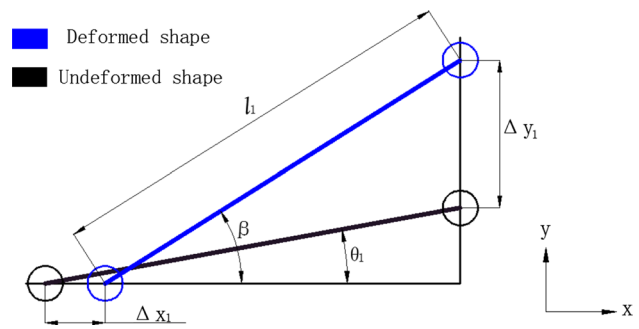


Fig. 5 The schematic of one half of a V-beam amplification

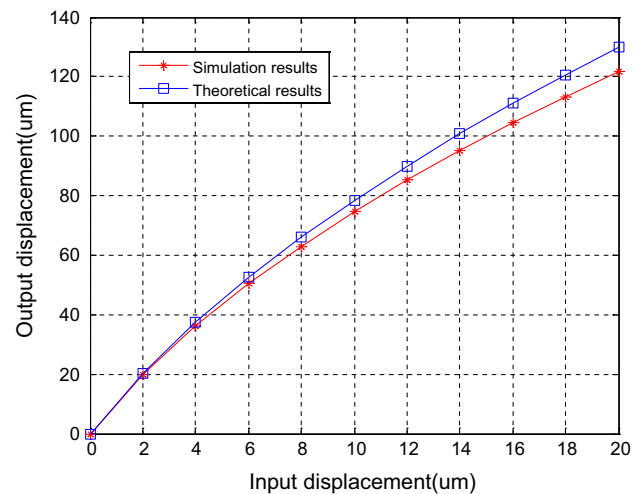


Fig. 6 The curves of the output displacement versus the input one

$w_1 = 10 \mu\text{m}$, $\theta_1 = 0.0875 \text{ rad}$, $h_1 = 50 \mu\text{m}$). Figure 6 shows the curves of the output displacement versus the input one, where the maximum deviation between two curves is 6.25 %.

2.2.2 Vertical anti-acceleration stiffness of a V-beam amplification

The vertical anti-acceleration stiffness of a mechanical amplification is defined as follows:

$$K_M = \frac{ma}{v_{max}} \tag{6}$$

where m , a and v_{max} is the mass, vertical acceleration and maximum vertical deformation of the mechanical amplification, respectively.

A V-beam amplification can be simplified to a double-clamped beam. Thus, the vertical anti-acceleration stiffness of a V-beam amplification can be calculated by the following equation:

$$K_{VM} = \frac{4Ew_1h^3}{l_1^3} \tag{7}$$

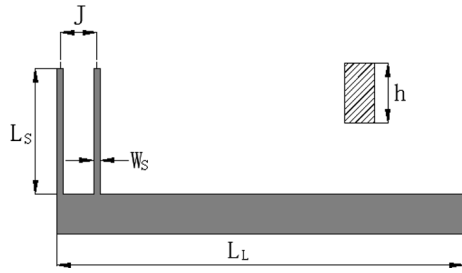
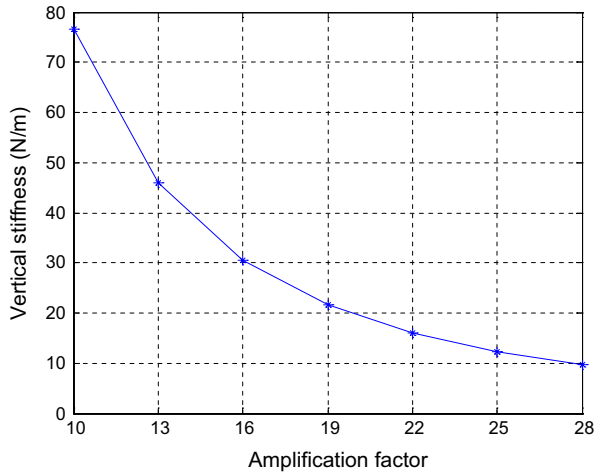
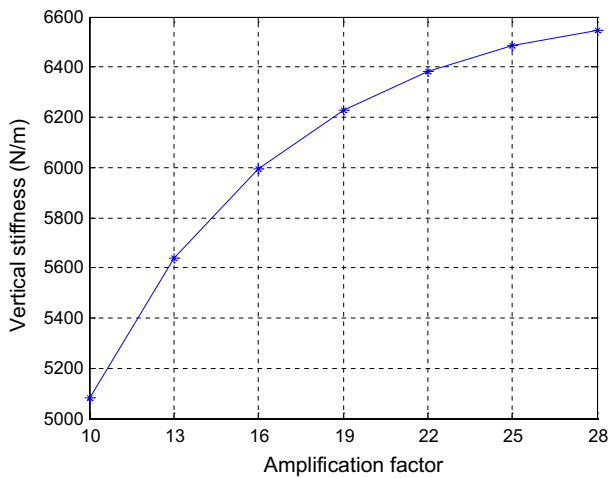


Fig. 7 The structure of a lever amplification



(a)



(b)

Fig. 8 a The vertical anti-acceleration stiffness of the lever amplification. b The vertical anti-acceleration stiffness of the V-beam amplification

The structure of a lever amplification is illustrated in Fig. 7. According to principle of equilibrium in mechanics, the vertical anti-acceleration stiffness can be obtained as:

$$K_{LM} = \frac{2\sigma J^2}{2L_L^2 + 2J^2 - 3L_L J} \tag{8}$$

where $\sigma = \frac{EW_S h^3}{4L_S^3}$.

Figure 8 shows the vertical anti-acceleration stiffness of the two different amplifications with specific size. It is obvious that the vertical anti-acceleration stiffness of V-beam amplifications is almost two orders of magnitude larger. Though the overall dimension of actual designs may vary, the vertical anti-acceleration stiffness of V-beam amplifications is still much larger than that of lever amplifications when the amplification factor is the same. Thus, actuators with V-beam amplifications are much more suitable for high-acceleration MEMS SA devices.

2.2.3 The input stiffness of a V-beam amplification

Linear behaviour is assumed and elementary bending theory is adopted when the input stiffness of a V-beam amplification is analyzed. Thus, the input stiffness of the first-stage V-beam amplification is obtained as:

$$k_{i1} = \frac{k_A k_T}{k_T \cos^2 \theta_1 + k_A \sin^2 \theta_1} \tag{9}$$

where $k_A = Ew_1 h/l_1$ and $k_T = Ew_1^3 h/l_1^3$.

The input stiffness of a cascaded V-beam amplification can be derived by theory of linear spring as:

$$k_{in} = \varepsilon^2 k_{i1}^2 k_{i2} \tag{10}$$

where $\varepsilon = \frac{n}{k_{i1}}$ and $n = \frac{l_1^2 - w_1^2}{l_1^2 \tan \theta_1 + w_1^2 \cot \theta_1}$. k_{i2} is the input stiffness of the second-stage amplification.

2.3 Combination of an electrothermal V-shape actuator with a cascaded V-beam amplification

The combination of an electrothermal V-shape actuator and a cascaded V-beam amplification can be regarded as the connection of two different springs as shown in Fig. 9.

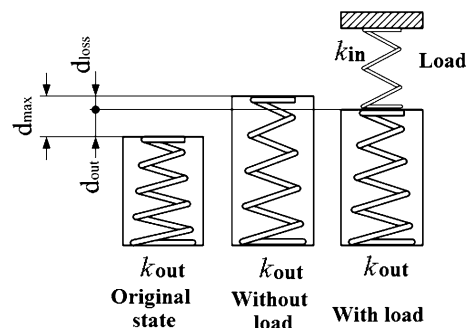


Fig. 9 The simplified model of the mechanism combination

The cascaded V-beam amplification acts as the load of the V-shape actuator and its input stiffness directly influences the output characteristics of the V-shape actuators. When the load is applied to the V-shape actuator, the output displacement loses partly and the actual displacement is:

$$d_{out} = \frac{1}{1+r} d_{max} \tag{11}$$

where $r = k_{in}/k_{out}$. k_{in} is the input stiffness of cascaded V-beam amplifications. d_{max} is the output displacement of V-shape actuators without load. The output energy E_{out} is used to represent the output capability of the V-shape actuator which can be expressed as:

$$E_{out} = \frac{1}{2} k_{in} d_{out}^2 = \frac{r}{(1+r)^2} \left[\frac{1}{2} k_{out} d_{max}^2 \right] \tag{12}$$

If $r < 1$, the output capability of the actuators is not fully used. However, the output energy is lost rapidly when $r > 1$. Taking safety factor into consideration, the total output stiffness of the 10-parallel V-shaped actuator in this paper is 271,380 N/m, which is larger than the input stiffness of the cascaded V-beam amplification of 46,013 N/m.

3 Device fabrication

The whole fabrication process of the device is shown in Fig. 10. Fabrication was performed on a SOI wafer with a device layer of 50 μm of Si, buried oxide of 3 μm and handle layer of 430 μm thick Si. The resistivity of the device layer is 0.01 ~ 0.02 Ωcm to provide a good electrical path of the MEMS device (Khawar et al. 2012). Firstly, bond pads were placed on the surface of the device layer by lift-off process. In order to obtain a good ohmic contact with the Si surface and stable pad surface for wire bonding, two layer structure of the pad was introduced—Cr/Au in 50/300 nm. Next, the proposed actuator design was patterned in photoresist (PR) aligned to both the cross-shaped mark and bond pads. AZ4620 photoresist was used to

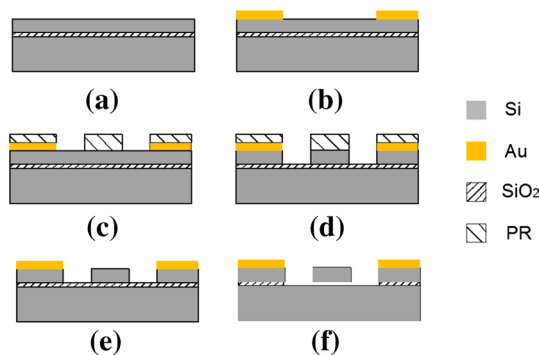


Fig. 10 The fabrication process of the device

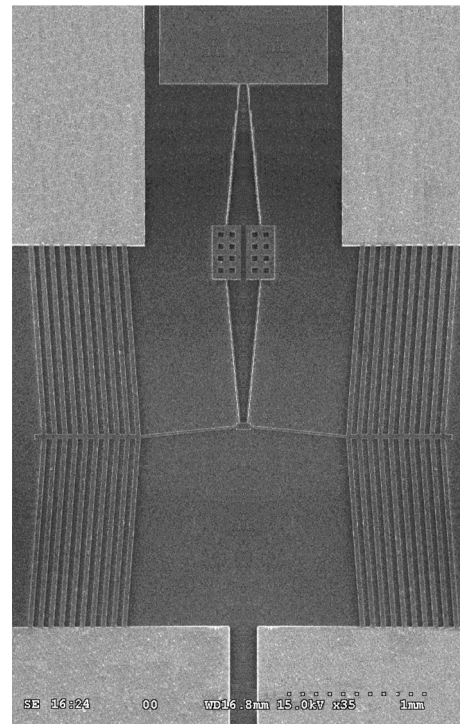


Fig. 11 A SEM photograph of the actuator for SA devices

make sure that the mask film was thick enough for etching. Next, the wafer was etched to the buried oxide layer by deep reaction ion etching. A large amount of PR could be removed by acetone after the process while the remains could be cleaned by oxygen plasma etching. Finally, the whole device was released by etching the buried oxide layer in HF liquid.

Figure 11 shows a SEM image of the actuator for SA devices fabricated on a SOI wafer.

4 Tests and results

4.1 Static characteristics of the actuator for SA devices

The displacements of the actuator under different voltages are shown in Figs. 12 and 13. The voltages applied on the actuator varies from 0 to 15 V, which can generate displacements from 0 to 231.78 μm. Under an applied voltage of 15 V, the simulation result of the displacement is about 271.60 μm. The deviation between experimental and simulation results is 14.66 %.

The relationship between the input power and displacement of the device is illustrated in Fig. 14, where the energy consumption is 5.10 W under 15 V.

The deviation between the measured and simulated displacement can be analyzed from the stiction between the

Fig. 12 The displacement of the device via a microscope. The applied voltages in **a** and **b** are 0 and 15 V, respectively

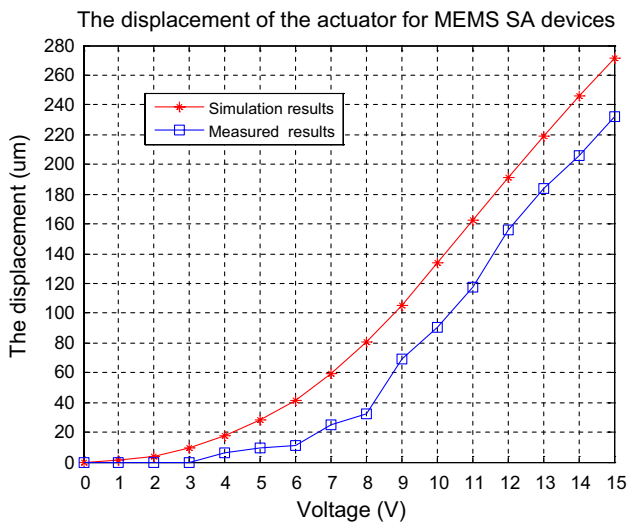
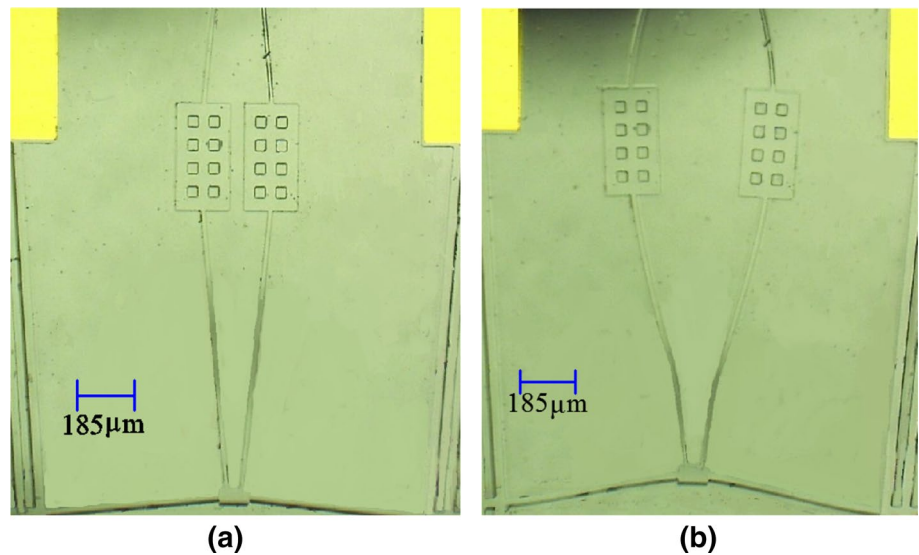


Fig. 13 The relationship between the displacement of the device and applied voltage

residual SiO₂ layer and device layer, which consumes the energy in the chip. The SiO₂ sacrifice layer may still remain in the gap between the movable parts and substrate more or less serving as the stiction source. The actuator for SA devices has a large surface because of the integrated mechanical slider, so the displacement deviation caused by stiction is obvious. The designed actuator would be more favorable and reliable for SA device if the internal stiction is alleviated by reducing the residual SiO₂ in structure release process.

4.2 Dynamic characteristics of the actuator for SA devices

In consideration that mechanical response time is far less than the thermal one, the dynamic characterization of the actuator is mainly determined by the thermal response time

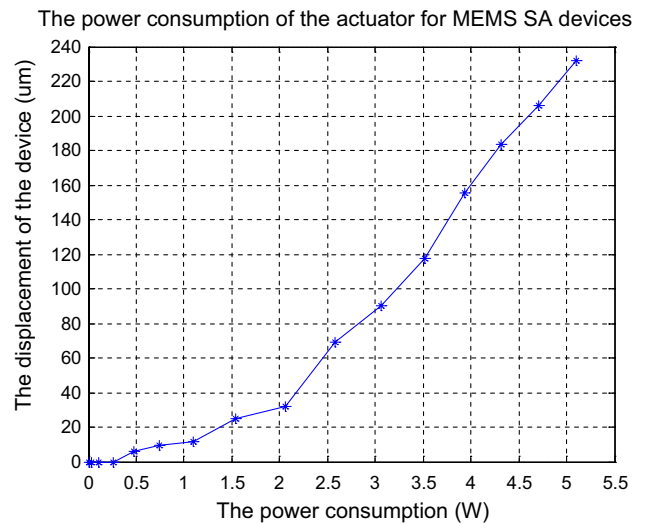


Fig. 14 The relationship between the input power and displacement of the device

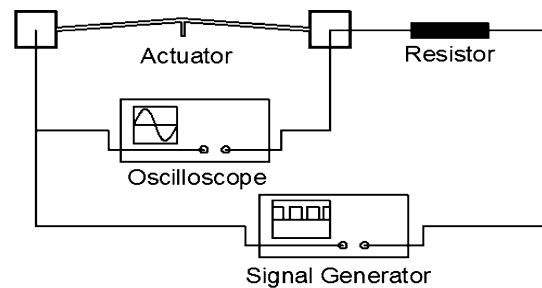


Fig. 15 Experimental setup for dynamic performance evaluation

of V-shape actuators. The resistance of Si could be constant only if the thermal distribution of electrothermal V-shape actuators reaches stability. Thus, the thermal response time

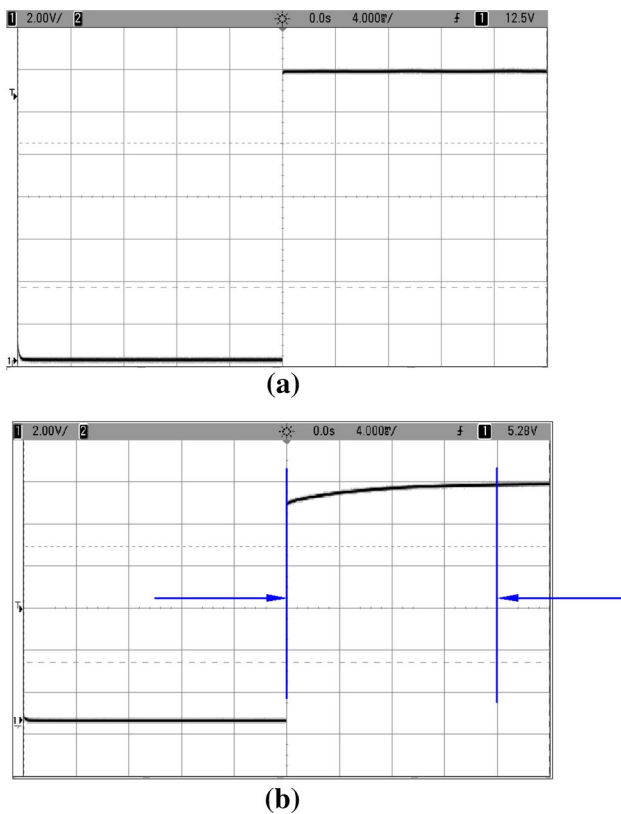


Fig. 16 **a** The voltage waveform of the square signal. **b** The voltage variation on the actuator

could be measured by the voltage variations on electrothermal V-shape actuators when a step voltage is applied. Figure 15 shows the experiment setup used for measuring the dynamic response time of the actuator. The setup is consisted of a signal generator, oscilloscope, resistor and the actuator. The signal generator provides a square signal with 40 ms in period, and the peak and valley values are 10 and 0 V, respectively. The actuator is connected to the signal generator through a resistor of 20 Ω . One channel of the oscilloscope is connected to the actuator to measure and record changes in applied voltage.

Figure 16a shows the voltage waveform of the square signal, where the peak waveform is flat. The voltage variations on the actuator under the square signal is illustrated in Fig. 16b. The waveform reaches the peak value gradually and the response time of the whole device is about 16 ms.

5 Conclusions

A large displacement thermal actuator with a cascaded V-beam amplification for MEMS SA devices is proposed, designed and fabricated. The device is comprised of two electrothermal V-shape actuators, a cascaded

V-beam amplification and two mechanical sliders. Compared with conventional lever amplifications, the vertical anti-acceleration stiffness of V-beam amplifications is much higher, which is fit for high-acceleration weapons. The amplification factor and input stiffness of a cascaded V-beam amplification are analyzed. Stiffness matching theory between an electrothermal V-shape actuator and a cascaded V-beam amplification is proposed and used to optimize the design. The special design of two symmetric mechanical sliders can double the displacement to ensure the MEMS SA device in armed state. The whole device is fabricated on a SOI wafer and fabrication process is introduced. Under an applied voltage of 15 V, the displacement of the device is 231.78 μm and the response time is about 16 ms with consuming power of 5.10 W. The chip size of the actuator is about 4 mm \times 5 mm \times 0.5 mm. The proposed actuator can be easily integrated with other sophisticated components of MEMS SA devices.

Acknowledgments This work is supported by the State Key Laboratory for Manufacturing System Open Research Fund (No. sklms2013002) and Key Laboratory Foundation of General Armament Department (No. 9140C370205130C37138).

References

- Deuschinger A, Schmid U, Schneider M, Brenner W, Wanzenböck H, Volland B, Ivanov T, Rangelow I (2010) Characterization of an electro-thermal micro gripper and tip sharpening using FIB technique. *Microsyst Technol* 16(11):1901–1908
- Enikov ET, Kedar SS, Lazarov KV (2005) Analytical Model for Analysis and Design of V-shaped thermal microactuators. *J Microelectromech Syst* 14(4):788–798
- Fan L, Last H, Wood R, Dudley B, Khan MC, Ling Z (1998) SLIGA Based underwater weapon safety and arming system. *Microsyst Technol* 4(4):168–171
- Gianchandani YB, Najafi K (1996) Bent-beam strain sensors. *J Microelectromech Syst* 5(1):52–58
- Hélène P, Carole R, Marjorie S, Fabrice M, Xavier D, Samuel C, Ludovic S, Véronique C (2010) Integration of a MEMS based safe arm and fire device. *Sens Actuators A* 159(1):157–167
- Hill D, Szyzkowski W, Bordatchev E (2006) On modeling and computer simulation of an electro-thermally driven cascaded nickel micro-actuator. *Sens Actuators A* 126(1):253–263
- Khawar A, Seyedhamidreza A, Zayd CL (2012) Design and characterization of a low temperature gradient and large displacement thermal actuators for in situ mechanical testing of nanoscale materials. *J Micromech Microeng* 22(1):1–12
- Khazaai JJ, Haris M, Qu H (2010) Displacement amplification and latching mechanism using V-shape actuators in design of electrothermal MEMS switches. *Proc IEEE Conf Sens* 27:1454–1459
- Lai Y, Bordatchev Evgueni V, Nikumb Suwas K, Hsu Wensyang (2006) Performance characterization of in-plane electro-thermally driven linear microactuators. *J Intell Mater Syst Struct* 17(1):919–929
- Long Q, Jae-Sung P, Gianchandani YB (2001) Bent-beam electrothermal actuators-part I: single beam and cascaded devices. *J Microelectromech Syst* 10(2):247–254

- Maloney JM, Schreiber DS, DeVoe DL (2004) Large-force electrothermal linear micromotors. *J Micromech Microeng* 14(2):226–234
- Maurer WH, Soto GH, Hollingsworth DR (2006) MEMS safe arm device for microdetonation. US Patent 7040234 B1, 9 May
- Pennarun P, Rossi C, Esteve D, Conedera V (2005) Development of MEMS based safe electro-thermal pyrotechnic igniter for a new generation of microfuzes. *Proc SPIE* 5836:558–569
- Pustan M, Rochus V, Golinval JC (2012) Mechanical and tribological characterization of a thermally actuated MEMS cantilever. *Microsyst Technol* 18(3):247–256
- Robinson CH, Wood RH, Hoang TQ (2005) Miniature MEMS-based electro-mechanical safety and arming device. US Patent 6964231 B1, 15 Nov
- Su X-PS, Yang Henry S (2001) Design of compliant leverage mechanisms. *Sens Actuators A* 87(1):146–156
- Yang Y-S, Lin Y-H, Hu Y-C, Liu C-H (2009) A large-displacement thermal actuator designed for MEMS pitch-tunable grating. *J Micromech Microeng* 19(1):1–12
- Zunino IJL, Skelton DR, Robinson C (2008) Reliability testing and analysis of safing and arming devices for army fuzes. *Proc SPIE* 6884:0C1–0C12